Uranium removal from aqueous solutions by adsorption on Aleppo pine sawdust, modified by NaOH and neutron irradiation

S. Menacer[a,*], A. Lounis[b], B. Guedioura[c], N. Bayou[a]

[a]Department of Management and Treatment of Radioactive Waste, Nuclear Research Center of Draria/Nuclear Safety Division and Radioprotection, BP 43, Sébala, Draria, Algeria, Tel. +213 774002322; email: saliaoui@yahoo.com (S. Menacer),
Tel. +213 21310358/61; email: naima_bayou@yahoo.fr (N. Bayou)
[b]Laboratory of Material Science and Engineering, University of Sciences and Technology Houari Boumediene, BP 32, El Alia, Bab Ezzouar, Algiers, Algeria, Tel. +213 698 700 920; email: zlounis@yahoo.com
[c]Nuclear Research Center of Draria/Nuclear Reactor Division, BP 43, Sébala-Draria, Algeria, Tel. +21321310358/61; email: algeryfx@yahoo.fr

ABSTRACT

Adsorption of uranium ions from aqueous solutions onto Aleppo pine sawdust was carried out in this study. This adsorbent is untreated, modified with NaOH, and neutron irradiated. The parametric study of uranium(VI) adsorption from aqueous solution onto untreated Aleppo pine sawdust has been investigated using batch equilibrium method at 293 K. The removal efficiency is studied as function of the effect of pH, adsorbent ratio, and contact time. A maximum adsorption capacity was obtained at pH 5 with an adsorbent ratio of 1 g/100 and an equilibrium time of 120 min for all the initial used concentrations. The kinetics of the adsorption process followed a second-order adsorption and the biphasic nature of the plot for intraparticle diffusion, showed diffusion through a film that is followed by a diffusion in the pores. The thermodynamic constants obtained at different temperatures, such as ΔG°_{ads}, ΔH°_{ads}, and ΔS°_{ads} suggested that the adsorption process is exothermic and spontaneous. In order to compare the adsorption capacities, both NaOH-treated and neutron-irradiated Aleppo pine sawdust were used for uranium(VI) adsorption using the optimal parameters obtained previously. Changes in physicochemical properties of the modified adsorbents were observed with FTIR and scanning electron microscope analyses. Adsorption tests showed that both treated sawdusts gave adsorption capacities better than the untreated sawdust. Four equilibrium models (Langmuir, Freundlich, Dubinin–Radushkevich, and Temkin) were applied to the experimental data in order to determine the better model for the systems. Langmuir isotherm seems the most appropriate for the adsorption of uranium(VI) with maximum adsorption capacities of 19.56, 48.66, 35.15, and 30.98 mg/g for the untreated, treated with NaOH, and neutron-irradiated (1 H and 4 H) sawdust, respectively.

Keywords: Sawdust; Wastes; Neutron irradiation; Adsorbent modified; Adsorption; Isotherm; Kinetic; Thermodynamic; Uranium

*Corresponding author.

1. Introduction

Different activities in industry and research laboratories give an excessive amount of radioisotopes through effluents which require appropriate management and treatment according to the international procedures and regulations [1]. Uranium appearing to be the most important heavy metal because of its high chemical toxicity and radioactivity that causes a public health problem even at very low concentrations. A lot of research efforts are concentrated on finding methods to remove this ion from aqueous solutions [2,3] and several techniques, such as coagulation and precipitation [4], ion exchange [5,6], are available in the literature. Adsorption is a cost-effective technique, simple to operate, and seems to be the appropriate treatment for effluents containing heavy metals ions [7].

Many natural or synthesized adsorbents are used for the removal of uranium(VI) [8–10]. According to Bailey [11], an adsorbent is estimated to be profitable if it is abundant in nature, agricultural wastes, or natural minerals and at low cost. Agricultural wastes are considered as good adsorbents because of two facts: they are renewable sources and low-cost materials. Furthermore, sawdust is not only abundant in the nature but also the most efficient and promising adsorbent in the removal of heavy metals [12,13].

Aleppo pine tree constitutes the major part of the Mediterranean forest surface area (about 3.5 million hectares). Particularly, in Algeria, surface area occupied by this tree is about 80,000 hectares which represents 35% of the wooded surfaces in the North of Algeria. Studies showed that treatment of wood sawdust, chemically or other should increase active sites on the surface of the adsorbent, which increases the adsorption capacity [7,12,14].

Irradiation by fast neutrons can be used in order to modify the chemical structure, microstructure, and properties of an organic material [15]. The radiation damage event is defined as the energy transfer from an incident projectile (fast neutrons and γ) to the solid resulting to a distribution of target atoms after completion of the event. This event is actually composed of several distinct processes: Transfer of energy from the neutron to the organic material can lead to the breaking of chemical bonds, free radical generation, and cross-linking formation [16,17]. Gamma irradiation induces both heating (resulting from gamma–photon energy absorption) and formation of free radicals. Consequently, the degree of damage, inflicted upon the matrix is dependent on the irradiation characteristics such as irradiation time in a particular reactor facility.

Porous solids have already proven approaches for adsorption. The chemical composition of these mesoporous materials allows intrinsic properties for the extraction, and therefore functionalization becomes unnecessary. Overall, examples of separation of radioactive elements by functional mesoporous materials are based on oxide matrices. These adsorbents have a thermal, chemical, and mechanical stability limited in the conditions of their nuclear use (strong acidity, high ionic strength, irradiation etc.) [18,19]. To overcome these limitations, we should be able to implement carbon-based matrices. Irradiation is one of the new functionalization ways for these innovative matrices, and their use in the treatment of nuclear wastes should be considered.

The aim of this work is to improve the adsorption of uranium(VI) onto Aleppo pine sawdust both untreated, modified chemically, and by neutron irradiation. Parameters influencing the adsorption, such as absorbent dosage, pH of adsorbate solution, and contact time, are studied for the untreated sawdust. In order to understand the nature of the adsorption, three sorption kinetic models (pseudo-first-order, pseudo-second-order, and intraparticle diffusion) were tested.

2. Materials and methods

2.1. Materials

Aleppo pine sawdust obtained from a local timber was washed three times with distilled water to remove impurities and then dried in an oven at 50°C for 48 h, finally ground and sieved through a range of sieves.

The chemical composition of the sawdust dried and ash free was carried out according to the standard protocols of TAPPI norms (Technical Association of the Pulp and Paper Industry).

All chemicals used in this work were products for analysis from Merck (Germany) and have not undergone any prior purification. A stock solution of uranium (1 g/L) was prepared by dissolving an accurate weight of uranyl nitrate ($UO_2(NO_3)_2$, $6H_2O$) (99%, Merck) in distilled water. The average particle diameter of the particle size fraction is analyzed with the Malvern Mastersizer 2000 type. The point of zero charge (pHzc) of the Aleppo pine sawdust provides information on the adsorption mechanism of uranium (VI) and was carried out according to the method described in our previous work [20]. Ion exchange and acidic properties of Aleppo pine sawdust were investigated using the method described by Aravindhan et al. [21] with the objective to study the nature of the adsorption of the sawdust.
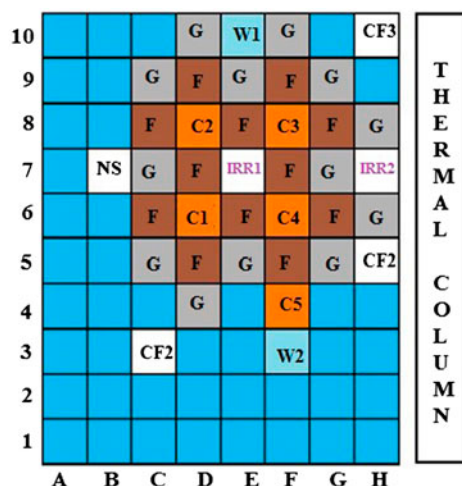
Fig. 1. Reflected configuration of irradiation in NUR reactor.

2.1.1. Sawdust treated by irradiation (SD$_{irra}$)

Sawdust is irradiated at NUR Research Reactor (1 MW). This open-pool reactor comprises MTR fuel type in which 17 fuel assemblies are arranged in a rectangular lattice. Fuel elements and graphite moderator are assembled around the core in a cubical arrangement to obtain a fully reflected configuration as shown in Fig. 1. An aluminum box containing ten capsules is used for irradiation tests. The neutron irradiation was performed at a position H 7 (IRR2), where the maximum temperature, $T = 42°C$. The total neutron flux measured using a gold foil was $\Phi_{tot} = 4.2 \times 10^{11}$ n cm^{-2}s^{-1}. The fast neutron flux (1.4×10^{11} n cm^{-2}s^{-1}) was evaluated with a Cd-covered Indium foil based on ^{115}In (n, n´)^{115m} In reaction with neutron energy threshold of 1.2 MeV.

The amount of radioactivity in the flux monitors was measured through gamma-ray spectrometry using germanium detector and spectrum analyzer linked to a PC.

Subsequently, the neutron flux to which the flux monitors had been exposed was calculated using the following formula [22]:

$$\phi = \frac{\lambda \times A \times M}{N \times \sigma_{eff} \times m \times \varepsilon \times \theta \times \gamma(1 - e^{-\lambda t_i})e^{-\lambda t_w}(1 - e^{-\lambda t_c})}$$

(1)

where ϕ is the thermal neutron flux, λ is the decay constant, A the gamma peak area, M the average atomic mass, and N is the number of nuclei/mol (equal to Avogadro's number), σ_{eff} the effective activation cross section, m the weight of the sample, ε the efficiency coefficient, θ the isotopic abundance, γ the intensity of the gamma photon, t_i the neutron irradiation time, t_w the waiting time between neutron activation and spectrometry measurement, and t_c the spectrometry measurement time.

Six samples (three for each fluency) were separately inserted in a well-sealed container and irradiated at two different fast neutron fluencies (4.5×10^{14} n cm^{-2} and 1.8×10^{15} n cm^{-2}), respectively.

2.1.2. Sawdust treated chemically by NaOH (SD$_{NaOH}$)

SD$_{NaOH}$ was prepared by stirring 20 g of sawdust in 1,000 mL of 0.1 M NaOH solution at 200 rpm for 60 min. Then the solution was filtered. The cake was washed several times with distilled water to remove the excess of NaOH until neutral pH. The obtained adsorbent is dried at 50°C overnight.

2.2. Batch study

Adsorption experiments were conducted in batch at 293 K, by stirring an accurate weight of Aleppo pine sawdust into 20 mL of a synthetic uranyl nitrate solution. All experiments were duplicated and the averages represent the results obtained. The residual uranium balance is determined by a simple and sensitive spectrophotometric method based on the formation of a colored complex with Arsenazo III to the wavelength of 652 nm [23] using Optizen Pop spectrophotometer.

The effects of particle size of the sawdust, pH solution, and adsorbent mass on the adsorption capacity of UO_2^{2+} were carried out by varying one parameter at a time and using an initial uranium concentration of 150 mg/L.

The initial pH of the solution was adjusted within the range from 3 to 9 using 0.1 M NaOH and 0.1 M HNO$_3$. The solid/liquid ratio is determined by varying the adsorbent mass from 5 to 100 g of sawdust per liter of uranyl nitrate solution.

Kinetic studies were performed on four initial concentrations (50, 100, 150, and 200 mg/L) of uranium(VI) with varying contact time between 0 and 240 min for the untreated sawdust. The thermodynamic study of the adsorption of uranium onto untreated Aleppo pine sawdust is realized at the following three different temperatures: 293, 303, and 323 K in an isothermal shaker.

Equilibrium isotherms were determined by varying initial concentrations of uranium in the range of 50–350 mg/L for the untreated sawdust.

The adsorption capacity of uranium(VI) expressed in mg/g is given by the equation below:

$$q_e = (C_0 - C_t)V/m$$

(2)

where C_0 (mg/L) is the initial uranium concentration, C_t (mg/L) is the liquid-phase concentration of uranium at any time, V (L) is the volume of the solution, and m (g) is the mass of the used dry adsorbent.

2.2.1. Error analysis

Four error functions were used as a criterion for the adaptation of the theoretical models to experimental results [20].

The Root Mean Square Error (RMSE) is represented by the following equation:

$$RMSE = \sqrt{\frac{1}{n-2}\sum_{1}^{n}(q_i - q_{ie})^2} \tag{3}$$

The Chi-square test:

$$\chi^2 = \sum_{i=1}^{n}\frac{(q_i - q_{ie})^2}{q_{ie}} \tag{4}$$

The Sum of the Absolute Errors (SAE):

$$SAE = \sum_{i=1}^{n}|q_i - q_{ie}|_i \tag{5}$$

The Average Relative Error (ARE):

$$ARE = \frac{100}{n}\sum_{i=1}^{n}\left|\frac{q_i - q_{ie}}{q_i}\right| \tag{6}$$

where q_i (mg/g) is the experimental value of uptake, q_{ie} (mg/g) is the calculated value of uptake using a model, and n is the number of measurements.

The smaller values of the error analysis indicate the better curve fitting.

3. Results and discussion

3.1. Characterization of Aleppo pine sawdust

Table 1 represents the characteristics and the chemical composition of Aleppo pine sawdust. Similar characteristic results are reported in the literature [24].

Table 1
Characteristics and chemical composition of Aleppo pine sawdust

Density (g/mL)	0.167
Humidity (%)	6.73
Average diameter (μm)	644.81
Point of zero charge	5.5
[COO⁻] (mmol/g)	1.8
Ash (%)	0.38
Total lignins (%)	27.16
Extractives (%)	1.87
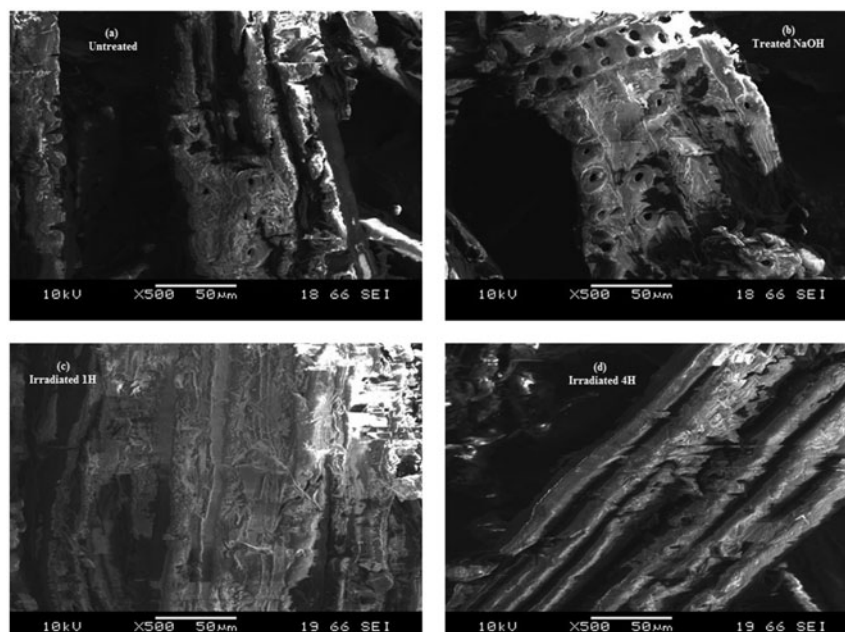
Fig. 2. SEM of Aleppo pine tree sawdust.
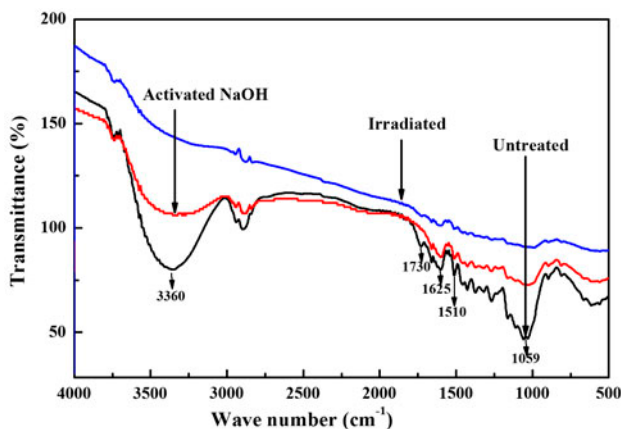
Fig. 3. FTIR spectrum of Aleppo pine sawdust.

Fig. 2 shows the structure of the surface of Aleppo pine sawdust both treated and untreated. We use a scanning electron microscope (Philips brand XL 30 ESEMFEG).

The different micrographies show a fibrous structure which is organized in a complex cell from the growth mechanism of Aleppo pine and cellulosic material remaining unchanged for all the samples. We also observe a juxtaposition of fibrils. The external surfaces are full of cavities in various shapes and sizes as well as a porosity varying from 20 to 50 μm.

The irradiated sample consists of a porous and heterogeneous structure possessing micropores, mesopores and macropores. The pores are directly oriented in parallel to the fiber axis. At the outer surface of the fibers, we observe furrows. This damage will result in two aspects, on one hand, the reduction of mass transfer and, on the other hand, a strong affinity of adsorbing UO_2^+ ions. The untreated samples of sawdust show a homogenous porous, largely microporous structure. The sawdust treated with NaOH comprises larger pores, due to the diffusion of hydroxyl ions.

Infrared analysis of the sawdust is carried out between 400 and 4,000 cm^{-1} using Nicolet-380 spectrum model. The FTIR spectra of Aleppo pine sawdust (Fig. 3) show that various functions have been affected by the treatment with NaOH as well as by neutron irradiation.

The absorption band at 1,510 cm^{-1} which is characterized by the bonding C=C of the aromatic ring of the lignin is significantly affected on the spectrum FTIR of the irradiated sawdust. This can be explained by the fact that the neutron scattering length has led to the surface damages already seen by SEM.

The mitigation of transmission on various absorption bands (3,360, 1,730, 1,625, and 1,059 cm^{-1}) is also observed due to the decrease of densities in carboxylic and phenol, carbonyl and hydroxyl groups, particularly in the irradiated sawdust.
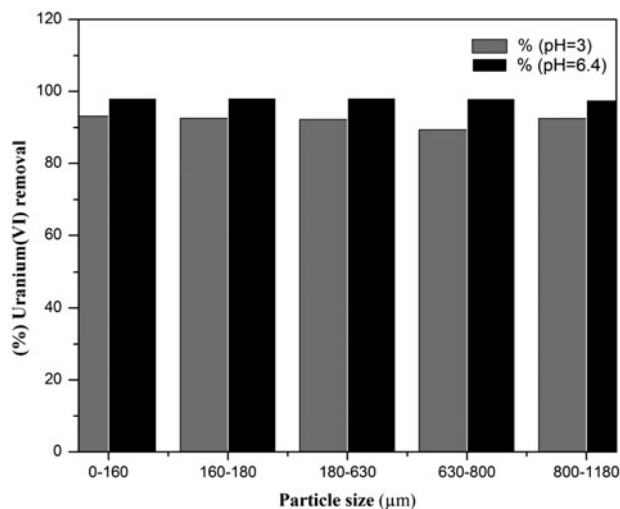
Fig. 4. Particle size effect.

3.2. Study of different parameters on the uranium adsorption onto Aleppo pine sawdust

3.2.1. Particle size effect

Fig. 4 shows the histogram of uranium adsorption depending on the particle size of the sawdust at pH 3 and 6.4 with an initial concentration of 150 mg/L, a contact time of 240 min, and an adsorbent dosage of 1/100 (g/mL). The fraction between 180 and 630 μm gave the best adsorption efficiency exceeding 98% for a pH of 6.4. This fraction was used for the remainder of the study.

3.2.2. Effect of the contact time and initial concentration of uranium(VI)

The balance in the study of the adsorption time is very important in determining the economic point of
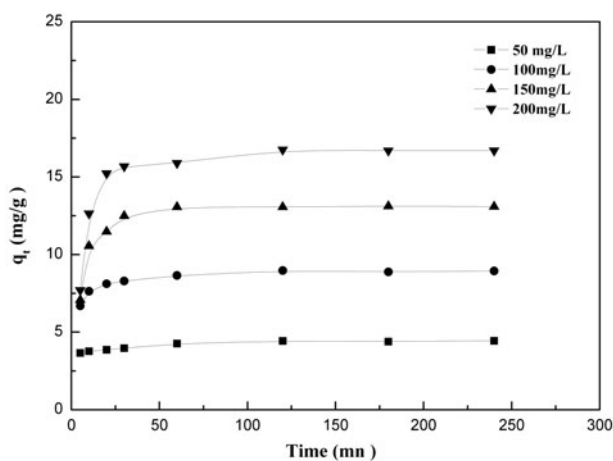
Fig. 5. Effect of initial concentration uranium(VI) and contact time.

view for the effluent treatment setting. The effect of contact time and initial concentration on the adsorption of UO_2^+ represented in Fig. 5 shows that the adsorption is very fast in the first 20 min of contact at all initial studied concentrations. This is due to the availability of active sites on the sawdust at the beginning of adsorption. The equilibrium time is reached after 120 min.

3.2.3. Effect of pH

The results of the adsorption equilibrium vs. pH are shown in Fig. 6.

The equilibrium increases from 8.30 mg/g at pH 3 to 12.62 mg/g at pH 5 and fall between pH 7 and 9. Since the surface of the adsorbent is negatively charged for pH values above 5.5 (pH$_{ZC}$ determined previously), and therefore it is likely to capture the positive ions, the adsorption capacity is maximum at pH 5 and it starts decreasing from pH 7.

To interpret these results, we should consider the neutral and ionic species in the solution. Different mononuclear and polynuclear uranium(VI) hydrolysis products in the form $[(UO_2)_p(OH)_q]^{(2p-q)+}$ as a function of pH values are present in the uranium solution. The repartition is determined by the following equilibria [25]:

$$pUO_2^{2+} + qH_2O \leftrightarrow \left[(UO_2)_p(OH)_q\right]^{(2p-q)+} \tag{7}$$

$$UO_2^{2+} + H_2O \leftrightarrow [UO_2(OH)]^+ + H^+ \quad pK = 5.20 \tag{8}$$

$$2UO_2^{2+} + 2H_2O \leftrightarrow [(UO_2)_2(OH)_2]^{2+} + 2H^+ \\ pK = 5.62 \tag{9}$$
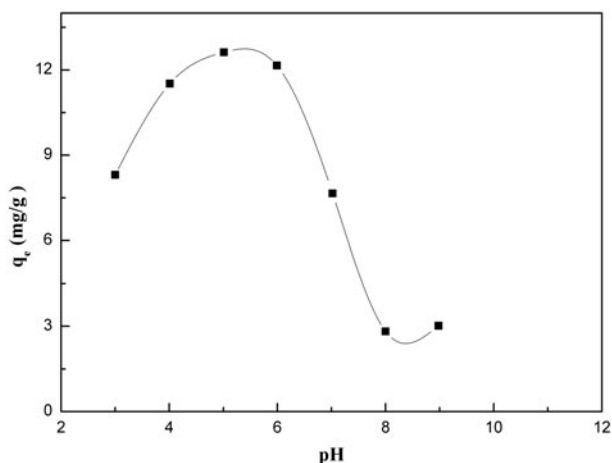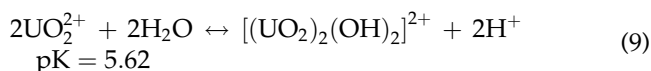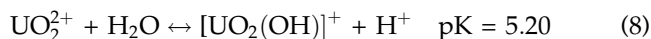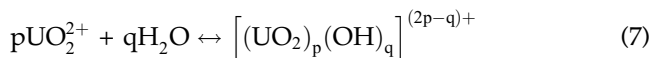
Fig. 6. Effect of pH on adsorption of uranium(VI).

$$3UO_2^{2+} + 4H_2O \leftrightarrow [(UO_2)_3(OH)_4]^{2+} + 4H^+ \\ pK = 11.90 \tag{10}$$

$$3UO_2^{2+} + 5H_2O \leftrightarrow [(UO_2)_3(OH)_5]^+ + 5H^+ \\ pK = 15.55 \tag{11}$$
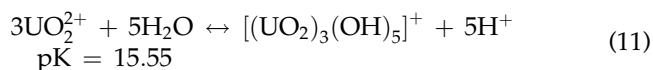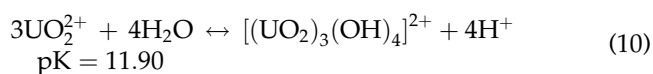
At pH between 3.0 and 5.0, the polynuclear products $[(UO_2)_2(OH)_2]^{2+}$, $[(UO_2)_3(OH)_4]^{2+}$, and $[(UO_2)_3(OH)_5]$ are present with UO_2^+ and $[UO_2(OH)]^+$) (Fig. 6), and are available for adsorption. At pH higher than 6, the hydrolysis is more intense and other polynuclear product, $[(UO_2)_4(OH)_7]^+$, is formed [26]. All these species can be readily adsorbed or ion exchanged by the sawdust. This observation can be explained by looking more closely to the functional groups of the surface of our material.

In our previous work, we have paid special attention to the analysis of plants as *Stipa tenacissima* (Esparto or Alfa is the Arab name), Diss (*Ampelodesmos Mauritanicus*) [27], and sawdust Aleppo Pine Tree [20]. The cell walls of these materials consist mainly of cellulose, lignin, and many hydroxyl groups such as tannins or other phenolic compounds. The absorption band at 3,360 cm^{-1} (Fig. 3) indicates that OH groups are not free but enter in various fashion OH stretching of hydrogen bonds. The peak at 1,059 cm^{-1} was assigned to C–O–C ether bending to allot coniferyl alcohol. All those components are active ion exchange compounds. Lignin, the third major component of the wood cell wall, is a polymer material. We have characterized this material by chromatography (GC/MS), HPL chromatography, and mass spectrometry analysis.

Lignin molecule is built up from the phenyl propane nucleus i.e. an aromat. Vanillin and syringaldehyde are the two other basic structural units of lignin molecule [27]. The value of pH$_{zc}$ was found to be 5.5 which indicates that the surface is negative and this helps to adsorb positively charged uranyl ion species through electrostatic interaction. Initially, the sawdust may be considered non-polar; in practice, the CO groups will complex in the presence of water which is a polar solvent.

A pH greater than 6, we cannot dismiss the fact that the $UO_2(OH)_2$ may be adsorbed by hydrogen bonding mechanism simultaneously with ion-exchange mechanism species. Also, we note that both mechanisms can be described by the following reactions:

Ion exchange

$$2(R - COH) + UO_2^+ \leftrightarrow (R - CO)_2U + 2H^+ \tag{12}$$
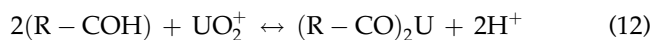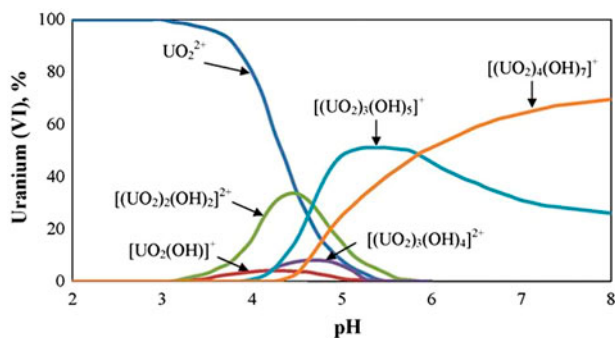
Fig. 7. Percentage species of uranium(VI) in a solution (10^{-3} M) vs. pH adapted by Misaelides et al. [26].

Fig. 8. Adsorbent mass effect on the adsorption of uranium(VI).

$$R - COH + UO_2(OH)^+ \leftrightarrow R - COUO_2OH + H^+ \quad (13)$$

$$\begin{aligned} 2(R - COH) &+ (\ UO_2)_2(OH)_2^+ \\ &\leftrightarrow (R - CO)_2(UO_2)_2(OH)_2 + 2H^+ \end{aligned} \quad (14)$$

Hydrogen bonding

$$2(R - COH) + UO_2(OH)_2 \leftrightarrow (R - COH)_2UO_2(OH)_2 \quad (15)$$
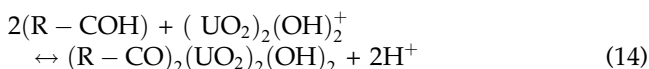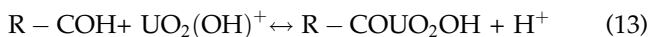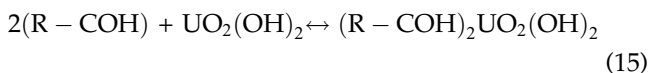
This explains the observed increase of uranium adsorbed at pH below 5.0. However, at pH of 6.0, a stable precipitation product $UO_2(OH)_2$ can be formed, and therefore the adsorption has to compete with the precipitation reactions. At pH higher than 6.0, the polynuclear species $(UO_2)(OH)^+$, $(UO_2)_2(OH)_2^{2+}$, and $(UO_2)_3(OH)_4^{2+}$ are not available anymore. The presence of species $(UO_2)_3(OH)_5^+$ are also limited until they finally disappear with an increasing pH (Fig. 7) [26]. Adsorption of uranium is limited at pH above 9 because no sufficient hydrolysis products are available at such a high pH, which explains the minimum adsorption of uranium at pH of 9 in Fig. 5. A pH value of 5 is retained for the rest of the work.

3.2.4. Adsorbent mass effect

Adsorbent mass effect on the adsorption capacity of uranium into Aleppo pine sawdust is represented in Fig. 8 for an initial concentration of uranium of 150 mg/L.

The adsorption capacity of UO_2^{2+} ions increases at equilibrium with the increase in the adsorbent mass until a solid/liquid ratio of 10 g/l, to remain more or less constant. By increasing the amount of adsorbent, the number of available adsorption sites increases indefinitely but does not affect the adsorption capacity. The equilibrium is reached at a concentration of 10 g/L. This ratio is held for the rest of the experiments.
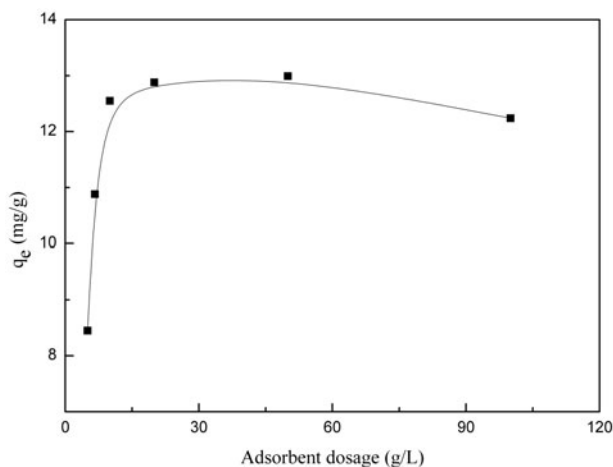
3.3. Kinetic studies

Three kinetic models as given in Table 2 (pseudo-first-order, pseudo-second-order, and intraparticle diffusion) [20] were used to fit the experimental data in the objective to determine the mechanism of adsorption and the potential rate controlling the different involved steps.

The best-fit selected model is based on the correlation coefficient (R^2), the calculated q_e values, and errors analysis (Table 3).

The second-order model showed the best fit to the experimental data for the four initial concentrations studied with correlation coefficients exceeding 0.99, and very low values error function compared to those found for the first-order kinetics. Moreover, the values of adsorption capacities calculated are very close to the experimental values found. The rate constant decreases as the initial uranium concentration increases.

In Fig. 9, the layout of the diffusion of the uranyl ions adsorption onto Aleppo pine sawdust is shown. This curve shows that the adsorption process is conducted in two phases which are linear paths for the four concentrations. The first step of adsorption is instantaneous on the outer surface and the second portion is the progressive adsorption step corresponding to the limiting step in the adsorption mechanism. As shown in Table 4, the rate constant of diffusion k_{id1} of the first step is higher than in the second step k_{id2}, inducing an increase in the diffusion resistance.

Table 2
Isotherm and kinetic models

Isotherm	Functional form	Plotting
Langmuir	$C_e/q_e = C_e/q_{max} + 1/bq_{max}$	C_e/q_e vs. C_e
Freundlich	$\ln q_e = \ln K_f + (1/n) \ln C_e$	$\ln (q_e)$ vs. $\ln (C_e)$
Dubinin–Radushkevich	$\ln q_e = \ln q_m - K_{DR}\varepsilon^2$	$\ln (q_e)$ vs. ε^2
Temkin	$q_e = B_T \ln (K_T) + B_T \ln (C_e)$	q_e vs. $\ln (C_e)$
Kinetics		
Pseudo-first-order	$\log (q_e - q_t) = \log (q_e) - (k_{1ads}\, t)/2.3$	$\log (q_e - q_t)$ vs. t
Pseudo-second-order	$t/q_t = 1/(k_{2ads}\, q_e^2) + t/q_e$	t/q_t vs. t
Intraparticle diffusion	$q_t = k_{id}\, t^{0.5} + C$	q_t vs. $t^{0.5}$

Table 3
Kinetic parameters of uranium(VI) adsorption and errors analysis

Model	Parameter	Initial uranium concentration (mg/L)			
		50	100	150	200
Pseudo-second-order	K_2	0.09	0.055	0.029	0.016
	$q_{e,cal}$ (mg/g)	4.48	9.014	13.285	17.015
	$q_{e,exp}$ (mg/g)	4.436	8.967	13.068	16.76
	R^2	0.999	0.999	0.999	0.999
	RMSE	0.295	0.152	0.706	1.000
	χ^2	0.168	0.019	0.334	0.573
	SAE	1.257	0.83	2.689	4.073
	ARE	4.143	1.353	3.960	5.124
Pseudo-first-order	K_1 (g/mg/mn)	0.016	0.016	0.086	0.019
	$q_{e,cal}$ (mg/g)	0.729	1.38	7.804	3.60
	R^2	0.953	0.950	0.96	0.89
	RMSE	4.35	8.61	5.3	14.27
	χ^2	250.62	552.48	7.89	453.08
	SAE	21.31	58.87	14.53	83.17
	ARE	89.40	89. 29	34.5	83.59
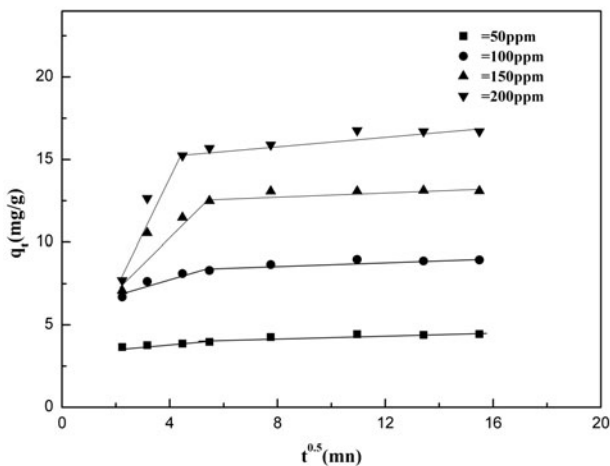
Fig. 9. Intraparticle diffusion plots for uranium(VI) adsorption.

Table 4
Intraparticle diffusion rate constants

Concentration (mg/L)	K_{id1} (mg/g/mn$^{1/2}$)	K_{id2} (mg/g/mn$^{1/2}$)
50	0.092	0.02
100	0.474	0.031
150	1.527	0.004
200	2.38	0.099

Uranium(VI) is first adsorbed by the outer surface with a relatively high rate of adsorption, until saturation, and then diffuses into the internal pores of the particles through the inner surface of the adsorbent. This is confirmed by the biphasic nature of the plot of the intraparticle diffusion.

3.4. Thermodynamic study

Thermodynamic parameters are essential in determining the nature of the retention process. Changes in the Gibbs free energy ($\Delta G°$), enthalpy ($\Delta H°$), and entropy ($\Delta S°$) for the adsorption process are obtained from the following equations [24]:

$$\ln K_D = \left(\Delta S°_{ads}\right)/R - \left(\Delta H°_{ads}\right)/RT \qquad (16)$$

$$\Delta G°_{ads} = \Delta H°_{ads} - T\Delta S°_{ads} \qquad (17)$$

From the coefficient distribution calculated by Eq. (17), all thermodynamic parameters are deduced from the plot ln (K_D) vs. $1/T$.

$$K_D\left(\text{ml/g}\right) = \left((C_0 - C_e)\,V\right)/(C_e\,m) \qquad (18)$$

where R is the ideal gas constant equal to 8.31 J/mol K, and T is the temperature in Kelvin.

The plot ln K_D vs. $1/T$ (Fig. 10) gives a straight line with slope $\Delta H°_{ads}/R$ and an intercept $\Delta S°_{ads}/R$. The values obtained are presented in Table 5.

The negative value of the Gibbs free energy indicates the feasibility and spontaneity of the adsorption process [25]. The negative value of $\Delta H°_{ads}$ suggests that the adsorption process is exothermic. In general, the change in enthalpy due to chemisorption is of 40–120 kJ/mol compared with the value of the enthalpy due to physical adsorption (<40 kJ/mol). Experimentally, it appears that the uranium adsorption onto Aleppo pine sawdust is physical (−14.61 kJ/mol). However, the fact that the pseudo-second-order kinetic obtained based on an adsorption capacity rather provides the validity of chemisorption which controls the kinetics [21], Aleppo pine sawdust seems involving also, ion exchange in the adsorption.

$\Delta S°_{ads}$ value obtained was positive and can be explained by the redistribution of energy between the adsorbent and the adsorbate. The distribution of energy of rotation and translation between molecules should increase with the increase in adsorption by providing a positive value of $\Delta S°$. This further confirms that the adsorption is spontaneous and reflects the affinity between the adsorbent and the adsorbate [21].

3.5. Equilibrium isotherms of UO_2^+ onto the untreated and treated sawdust

Experimental adsorption isotherms of uranium onto untreated and treated sawdust are represented in Fig. 11. The results show that the maximum experiment adsorption capacity does not exceed 18.52 mg/g at equilibrium for the untreated sawdust,

Fig. 10. Graphical determination of $\Delta H°_{ads}$ and $\Delta S°_{ads}$.
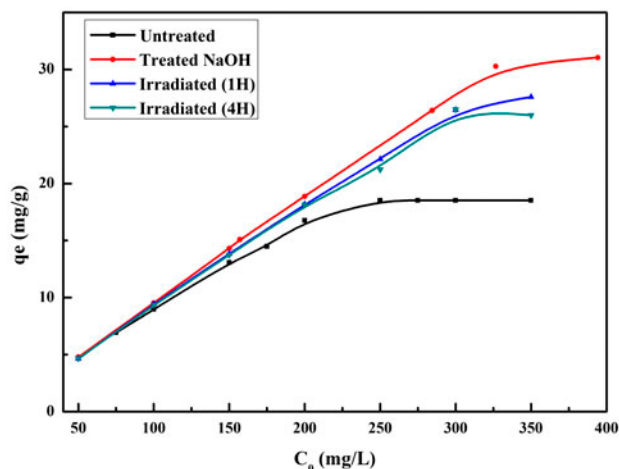
Fig. 11. Equilibrium isotherms of UO_2^{+t} onto the untreated and treated sawdust.

Table 5
Thermodynamic parameters of uranyl ions adsorption by Aleppo pine sawdust

Initial concentration (mol/L)	R^2	ΔH_{ads} (kJ/mol)	ΔS_{ads} (J/mol K)	$\Delta G°_{ads}$ (kJ/mol)		
				293 K	303 K	323 K
0.63×10^{-3}	0.99	−14.61	4.17	−15.83	−15.87	−15.95

Table 6
Isotherms parameters of uranium(VI) adsorption and errors analysis for the untreated and treated sawdust

	Model	Langmuir	Freundlich	Temkin	Dubinin–Radushkevich
Untreated sawdust	q_{max} (mg/g)	19.95			
	b (L/mg)	0.11			
	K_f (mg$^{(1-1/n)}$/g/L$^{1/n}$)				
	n		4.88		
	K_T (L/mg)		3.38		
	B_T			1.47	
	q_m (mg/g)			3.74	16.76
	K_{DR}				6.42
	R^2	0.991	0.86	0.90	0.83
	RMSE	0.95	2.15	1.46	15.75
	χ^2	0.49	2.05	1.02	44.16
	SAE	6.41	14.29	9.78	68.46
	ARE	5.66	11.02	7.99	90.71
Treated sawdust with NaOH	q_{max} (mg/g)	48.66			
	b (L/mg)	0.059			
	K_f (mg$^{(1-1/n)}$/g/L$^{1/n}$)				
	n		3.78		
	K_T (L/mg)		1.57		
	B_T			0.65	
	q_m (mg/g)			10.30	
	K_{DR}				23.23
	R^2				1.93
	RMSE	0.981	0.94	0.98	0.793
	χ^2	1.29	3.82	1.55	8.83
	SAE	0.06	3.08	1.58	20.92
	ARE	7.05	18.32	9.31	53.34
		6.04	12.61	10.38	39.96
Neutron-irradiated sawdust (1H)	q_{max} (mg/g)	35.15			
	b (L/mg)	0.0574			
	K_f (mg$^{(1-1/n)}$/g/L$^{1/n}$)		3.03		
	n		1.74		
	K_T (L/mg)				
	B_T			0.55	
	q_m (mg/g)			7.98	
	K_{DR}				22.23
	R^2				4.60
	RMSE	0.97	0.90	0.97	0.92
	χ^2	1.539	4.26	1.62	7.65
	SAE	0.787	3.51	0.63	15.92
	ARE	6.685	19.31	7.14	39.74
		8.02	17.45	6.56	55.63
Neutron-irradiated sawdust (4H)	q_{max} (mg/g)				
	b (L/mg)	30.98			
	K_f (mg$^{(1-1/n)}$/g/L$^{1/n}$)	0.0677			
	n		3.23		
	K_T (L/mg)		1.89		
	B_T			0.624	
	q_m (mg/g)			7.071	20.70
	K_{DR}				3.94
	R^2	0.98	0.89	0.92	0.86
	RMSE	2.254	4.88	2.49	7.16
	χ^2	1.31	4.74	1.43	14.36
	SAE	8.97	21.37	11.04	37.30
	ARE	8.2	17.42	8.57	49.81

Table 7
Capacities adsorption of different adsorbents used in the removal of uranium

Adsorbent	Adsorption capacity (mg/g)	Refs.
Aleppo pine sawdust	18.52	This study
Aleppo pine sawdust treated with NaOH	31.04	This study
Aleppo pine sawdust irradiated (1 H)	27.58	This study
Aleppo pine sawdust irradiated (4 H)	25.99	This study
Chitosan-triplyphosphate (CTTP) beads	239.9	[9]
Natural zeolite material	8.70	[26]
Activated carbon prepared from charcoal	28.5	[29]
Bentonite	238	[30]
MOCZ	15.1	[31]

where the maximum adsorption capacities are, respectively, 31.04, 27.58, and 25.99 mg/g for NaOH and neutron irradiated sawdust (1 H and 4 H) with a gradual saturation of the adsorbent. All the relevant remarks for the interpretation of SEM and FTIR are justified by the adsorption tests. It is also observed that the irradiated sample during 60 min has an adsorption better than that irradiated for 4 h. At this stage (irradiation for 4 h), the polymer cross-linking reaction is therefore achieved.

There is a critical threshold of irradiation beyond which fast neutrons and very high energy gamma rays (8 MeV), irrespective of thermal heating, the sample degradation is being observed. However, this damage can be regarded as a split mechanism and the multitude micro fragments obstruct the micropores. These comments enable us to anticipate how the adsorption phenomena should be tackled in terms of physisorption.

The isotherm obtained with NaOH treatment shows the increase in the negative charge over the surface which is due to the presence of OH^- ions, therefore, increases the electrostatic force of van Der Waals between the carbon surface and the UO_2^+ ions which increase uranyl ions adsorption. Furthermore, all the curves show an "L-shape", according to the Giles classification [28].

Experimental data were applied to Langmuir, Freundlich, Temkin, and Dubinin–Radushkevich models [20] as given in Table 2.

Table 6 shows the models' parameters with their respective correlation coefficients and the error calculation.

Langmuir isotherm is the best-fitted model used in the adsorption of UO_2^{2+} ions onto untreated sawdust with maximum adsorption capacities of 19.56, 48.66, 35.15, and 30.98 mg/g with correlation coefficients exceeding 0.97and low values of error functions.

The Freundlich constants (n) gave values of 3.38, 1.57, 1.74, and 1.89 for the untreated, NaOH-treated and irradiated (1 H and 4 H) sawdust, respectively. These

values indicate the acceptance of the mediums as suitable adsorbents, where UO_2^+ can be removed from aqueous solutions. Note also that n must be between 1 and 10 to classify the process as a favorable adsorption [9]. The isotherm obtained with irradiated sawdust during 4 h suggests, therefore, that the UO_2^+ ions' multi-layer adsorption is an opportunity not to exclude.

4. Conclusion

Performance of adsorbents is based on the maximum adsorption capacity of the adsorbent under favorable experimental conditions. Table 7 illustrates the comparison between adsorption capacities of different adsorbents in the removal of uranium.

By comparing these results, both treated and untreated Aleppo pine sawdust seem to be very efficient and effective way to eliminate uranyl ions since the adsorption capacity values are more or less important with the fact that it is an available source and low-cost material.

Langmuir model is the most appropriate for all the adsorbents.

The conventional adsorbents, like activated carbon and zeolites which both require alternative regeneration and synthesis, are economically unprofitable. Moreover, zeolites induce solid radioactive waste which cannot be incinerated.

The incineration of the solid radioactive waste, obtained after adsorption by the sawdust reduces strongly the effluents that contain uranium.

References

[1] IAEA Safety standards, Classification of radioactive waste—General safety guide, GSG-1, 2009.
[2] X. Shuibo, Z. Chun, Z. Xinghuo, Y. Jing, Z. Xiaojian, W. Jingsong, Removal of uranium(VI) from aqueous solution by adsorption of hematite, J. Environ. Radioact. 100 (2009) 162–166.

[3] S. Chabalala, E.M.N. Chirwa, Removal of uranium(VI) under aerobic and anaerobic conditions using an indigenous mine consortium, Miner. Eng. 23 (2010) 526–531.

[4] U. Forstner, G.T.W. Wittmann, Metal Pollution in the Aquatic Environment, second ed., Springer, New York, NY, 1983.

[5] C. Sarzanini, E. Mentaasti, V. Porta, Ion Exchange for Industry, Ellis Horwood, Chichester, UK, 1988, pp. 189–193.

[6] A. Lounis, L. Setti, A. Djennane, R. Melikchi, Electroextraction of molybdenum from a solution containing uranium by a process combining ion exchange resin and membranes, J. Appl. Sci. 7 (2007) 196.

[7] W.S. Wan.Ngah, M.A.K.M. Hanafiah, Removal of heavy metal ions from wastewater by chemically modified plant wastes as adsorbents: A review. Bioresour. Technol. 99 (2008) 3935–3948.

[8] R. Donat, The removal of uranium(VI) from aqueous solutions onto natural sepiolite, J. Chem. Thermodyn. 41 (2009) 829–835.

[9] M.K. Sureshkumar, D. Das, M.B. Mallia, P.C. Gupta, Adsorption of uranium from aqueous solution using chitosan-tripolyphosphate (CTPP) beads, J. Hazard. Mater. 184 (2010) 65–72.

[10] F. Houhoune, D. Nibou, S. Amokrane, M. Barkat, Modelling and adsorption studies of removal uranium (VI) ions on synthetized zeolite NaY, Desalin. Water Treat. 51 (2013) 5583–5591.

[11] S.E. Bailey, T.J. Olin, R.M. Bricka, D.D. Adrian, A review of potentially low-cost sorbents for heavy metals, Water Res. 33 (1999) 2469–2479.

[12] A. Shukla, Y.H. Zhang, P. Dubey, J.L. Margrave, S.S. Shukla, The role of sawdust in the removal of unwanted materials from water, J. Hazard. Mater. 95 (2002) 137–152.

[13] V. Mishra, C. Balomajumder, V.K. Agarwal, Biosorption of Zn(II) onto the surface of non-living biomasses: A comparative study of adsorbent particle size and removal capacity of three different biomasses, Water Air Soil Pollut. J. 211 (2010) 489–500.

[14] F. Gode, E.D. Atalay, E. Pehlivan, Removal of Cr(VI) from aqueous solutions using modified red pine sawdust, J. Hazard. Mater. 152 (2008) 1201–1207.

[15] G.S. Was, Fundamentals of Radiation Materials Science, Springer-Verlag, Berlin Heidelberg, 2007.

[16] B. Guedioura, N. Bendjaballah, N. Alioui, Profiling measurements of metal ion distribution in thin polymer inclusion membranes by Rutherford backscattering spectrometry, Radiat Eff. Defects Solids 169 (2014) 388–395.

[17] J.A. Cookson, Specimen damage by nuclear microbeams and its avoidance, Nucl. Instrum. Methods Phys. Res., Sect. B 30 (1988) 324–330.

[18] S. Le Caër, F. Brunet, C. Chatelain, D. Durand, V. Dauvois, T. Charpentier, J.P. Renault, Modifications under irradiation of a self-assembled monolayer grafted on a nanoporous silica glass: A solid-state NMR characterization, J. Phys. Chem. 116 (2012) 4748–4759.

[19] C. Delchet, A. Tokarev, X. Dumail, G. Toquer, Y. Barré, Y. Guari, Ch. Guerin, J. Larionova, A. Grandjean, Extraction of radioactive cesium using innovative functionalized porous materials, RSC Adv. 2 (2012) 5707–5716.

[20] N. Ouazene, A. Lounis, Adsorption Characteristics of Cl basic blue 3 from aqueous solution onto Aleppo pine sawdust, Color. Technol. 128 (2011) 21–27.

[21] R. Aravindhan, J.R. Rao, B.U. Nair, Removal of basic yellow dye from aqueous solution by sorption on green alga *Caulerpa scalpelliformis*, J. Hazard. Mater. 142 (2007) 68–76.

[22] F.A. Valente, Manual of Experiments in Reactors Physics, The Macmillan Company, New York, NY, 1963.

[23] W. Zou, L. Zhao, R. Han, Removal of Uranium(VI) by fixed bed ion-exchange column using natural zeolite coated with manganese oxide, Chin. J. Chem. Eng. 17(4) (2009) 585–593.

[24] M.E. Argun, S. Dursun, C. Ozdemir, M. Karatas, Heavy metal adsorption by modified oak sawdust: Thermodynamics and kinetics, J. Hazard. Mater. 141 (2007) 77–85.

[25] M.Z.-C. Hu, J.M. Norman, B.D. Faison, M.E. Reeves, Biosorption of uranium by *Pseudomonas aeruginosa* strain CSU: Characterization and comparison studies, Biotechnol. Bioeng. 51 (1996) 237–247.

[26] P. Misaelides, A. Godelitsas, A. Filippidis, D. Charistos, I. Anousis, Thorium and uranium uptake by natural zeolitic materials, Sci. Total Environ. 173–174 (1995) 237–246.

[27] S. Aroua, A. Lounis, F. Semaoune, S. Condom, Analysis of lignin isolated from alkaline leaching of alpha grass, Asian. J. Chem. 21 (2009) 2293–2300.

[28] C.H. Giles, D. Smith, A.J. Huitson, A general treatment and classification of the solute adsorption isotherm.I. Theoretical., J. Colloid Interface Sci. 47 (1974) 755.

[29] C. Kütahyalı, M. Eral, Selective adsorption of uranium from aqueous solutions using activated carbon prepared from charcoal by chemical activation, Sep. Purif. Technol. 40 (2004) 109–114.

[30] M.T. Olguin, M. Solache-Rios, D. Acosta, P. Bosch, S. Bulbulian, UO_2^{2+} sorption on bentonite, J. Radioanal. Nucl. Chem. 218 (1997) 65–69.

[31] R. Han, W. Zou, Y. Wang, L. Zhu, Removal of uranium(VI) from aqueous solutions by manganese oxide coated zeolite: Discussion of adsorption isotherms and pH effect, J. Environ. Radioact. 93 (2007) 127–143.